

IMAGE SEGMENTATION USING ROTATION-INVARIANT MULTILAYER COORDINATED CLUSTERS REPRESENTATION

Marcos J. Álvarez¹, Antonio Fernández¹, Elena González¹, Francesco Bianconi²,
Fernando J. Aguilar³ and Julia Armesto⁴

⁽¹⁾ *Universidade de Vigo*
ETSII, Departamento de Diseño en la Ingeniería
Vigo / Spain
E-mail: {marcos,antfdez,elena}@uvigo.es

⁽²⁾ *Università degli Studi di Perugia*
Dipartimento Ingegneria Industriale
Perugia / Italy
E-mail: bianco@unipg.it

⁽³⁾ *Universidad de Almería*
Escuela Politécnica Superior, Departamento de Ingeniería Rural
Almería / Spain
E-mail: faguilar@ual.es

⁽⁴⁾ *Universidade de Vigo*
ETSIM, Departamento de Ingeniería de Recursos Naturales y Medio Ambiente
Vigo / Spain
E-mail: julia@uvigo.es

Abstract

In this paper we propose the application of rotation-invariant multilayer Coordinated Clusters Representation (CCR) as a colour texture descriptor in image segmentation. Rotation-invariant multilayer CCR is a twofold improvement of the original CCR: on the one hand, the proposed features combine textural and colour information into a single model, and on the other hand, this image descriptor is robust against texture rotation. The central idea is to describe the colour content of an image by means of a reduced set of representative colours, and then to split the image into a stack of binary images, one for each colour of the reduced palette. In order to achieve rotation-invariance the original square window is replaced by a circular neighbourhood. The validity of the model has been demonstrated through the segmentation of both synthetic mosaics of OuTex textures and multispectral Ikonos-2 satellite images. Experimental results show that the proposed features have high discriminative power and yield increased accuracy compared to other segmentation methods.

Keywords: *colour texture, image segmentation, CCR*

1 INTRODUCTION

Eyesight is the most important and complex human sense. It provides a great amount of sensorial information that is processed by the brain and let us interact with the world around. This fact justifies the significance of computer vision –image analysis using computers– as a research field. Recent advances in imaging devices and computer processing power have made feasible a wide variety of computer vision applications, such as remote sensing, medical diagnosis, robot vision, process monitoring, quality control or security, to cite some.

Image segmentation –splitting an image into meaningful regions of homogeneous properties–

is a preprocessing stage in many computer vision applications. For image segmentation to be effective, a proper characterization of the input image is needed. Unfortunately, there does not exist a general purpose, universal approach to feature extraction, and therefore, the feature set depends on the nature of the information conveyed by the images to be processed.

Texture and colour are two of the most commonly used cues for image segmentation. These attributes have been traditionally regarded as separate phenomena. However, in recent years, fusion of colour and texture into a single model has re-

ceived a great deal of attention [3, 4, 5, 6, 7, 8, 13, 14, 16, 17, 22, 26, 27, 30].

Texture analysis techniques can be categorized into four families: statistical features, structural features, signal processing based features and model based features [28, 31]. Statistical texture features measure the spatial distribution of pixel values [12]. Structural features characterize texture through the occurrence frequency of certain texture primitives, and the spatial arrangement of these primitives. Signal based features are usually extracted by applying filter banks to the image and computing the energy of the filter responses [23]. Model based features generally characterize texture by the estimated parameters of the stochastic and generative models used to represent images.

The Coordinated Clusters Representation (CCR) is a binary texture descriptor that is halfway between statistical and structural methods. In this model a binary image is described by a histogram of occurrence of elementary binary texture patterns – called *texels*– which are defined over a square window. The set of all the possible texels constitutes a dictionary, in which each pattern is represented by a decimal code. For this method to be applied to gray-scale images, a prior global binarization is required. This is a major issue, since the use of an inappropriate threshold can wipe out textural information. Recently a robust CCR-based model has been proposed for colour texture classification [6]. This model, referred to as rotation-invariant multilayer CCR, yields a twofold improvement with re-

spect to the gray-scale CCR. First, the proposed descriptor combines colour and texture information; second, it is robust against changes in texture orientation. In addition, as this model is intended for colour texture rather than binary texture, there is no need to perform global thresholding because this troublesome task is replaced by colour indexing.

In this paper we propose the application of rotation-invariant multilayer CCR to image segmentation. The central idea is to describe the textural and colour content of an image by splitting the original colour image into a stack of binary images. Robustness against rotation is achieved by using circularly symmetric texels instead of the original 3×3 sliding window. To evaluate the performance of the proposed features we have applied this method to the segmentation of different colour and multispectral images. Experimental results show that rotation-invariant multilayer CCR features have a high discriminative power and yield increased accuracy with respect to other segmentation methods.

The remainder of this paper is organized as follows. In Section 2 we present the rotation-invariant multilayer CCR model for colour texture. Section 3 outlines the overall segmentation method. Section 4 details the benchmark data used in this article. Section 5 is devoted to describe the experimental results, and Section 6 summarizes the conclusions that can be drawn from this work.

2 COLOUR TEXTURE MODEL

2.1 CCR features

The Coordinated Clusters Representation (CCR) is a model that describes binary texture through the occurrence frequency of the possible binary patterns (texels) that can be defined over a square window [15]. The dimension of these elementary patterns is usually set to 3×3 pixels, since this size provides good discriminative power at a reasonable cost in terms of both computing speed and memory usage. In this case, the feature vector – denoted by $CCR_{3 \times 3}$ – has $2^9 = 512$ components. This binary texture descriptor was later extended to gray-scale texture images through thresholding [24, 25]. However, the need for global binarization is a major issue, since this preprocessing stage can degrade textural information. The choice of a proper binarization threshold is critical to preserve texture characteristics.

All the pixels in a 3×3 texel with a digital level greater or equal than the chosen binarization

threshold are assigned a digital value of 1. Besides, each of the 9 pixels is weighted by a power of 2. The $CCR_{3 \times 3}$ code is the sum of the weights of those pixels where the binarization takes a value of 1. It should be noticed that the weighting mask is arbitrary. Indeed, a different arrangement of the weighting factors would only result in a different coding of the patterns.

2.2 Rotation-invariant CCR

Sensitivity to texture orientation is another drawback of the CCR model. In practical applications it is important that features be invariant against rotation, since images are rarely captured under steady viewing conditions. Rotation-invariant CCR features can be obtained following an approach similar to the one proposed for the $LBP_{3 \times 3}$ operator [20].

The first step consists in replacing the squared

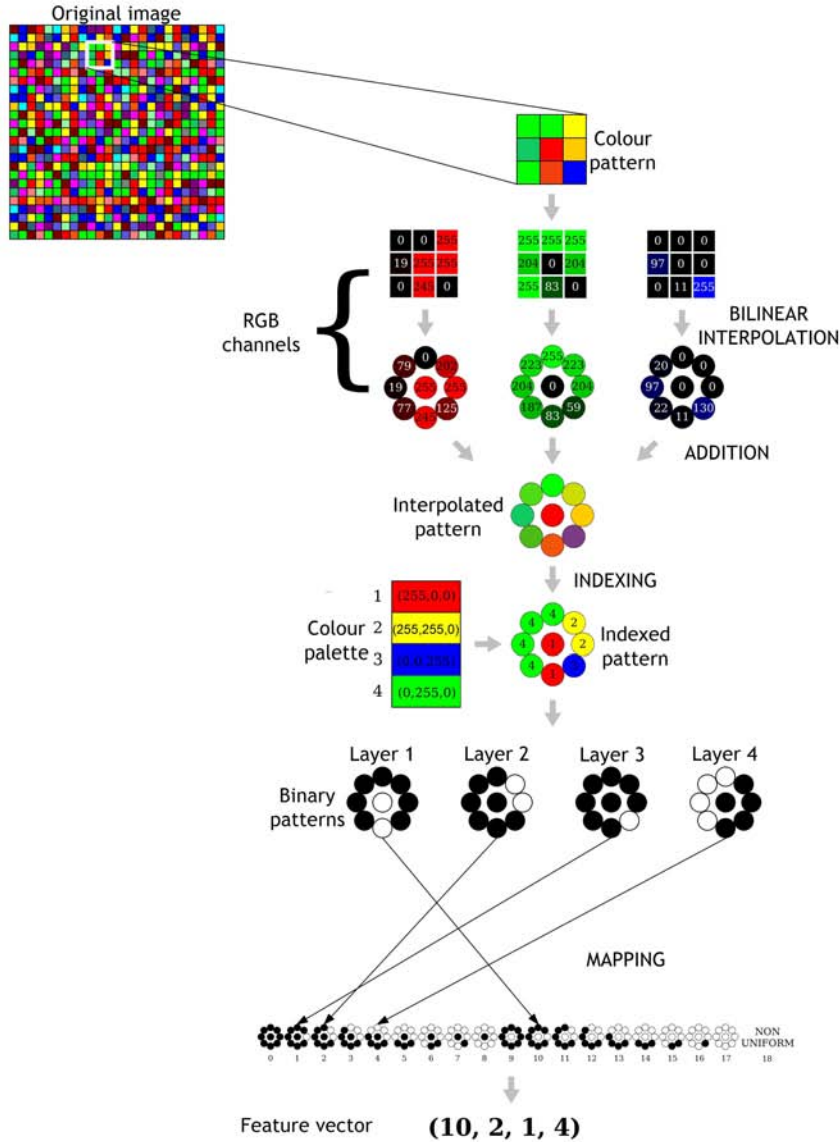


Figure 1: Schematic representation of the procedure to extract rotation-invariant multilayer CCR features

neighbourhood of the $CCR_{3 \times 3}$ by a circular one. The intensity of the pixels that are not placed exactly on pixels positions is estimated through bilinear interpolation. We denote this model by $CCR_{8,1}$.

In order to achieve rotation invariance, all those patterns that are rotated versions of the same pattern are mapped to the same primitive pattern. This descriptor—denoted by $CCR_{8,1}^{ri}$ —reduces the dimension of the feature space (i.e., the number of bins of the histogram) from 512 to 72 [10].

If we only consider the *uniform patterns*, i.e., those patterns where the number of transitions in the eight peripheral pixels is at most two, regardless of the value of the central pixel, a further reduction in the dimension of the feature space can be achieved. To be precise, there are 18 possible uniform texels in an 8-neighborhood of radius 1. The

remaining non uniform patterns are accumulated into an additional 19th bin. We refer to this feature space as the $CCR_{8,1}^{riu2}$.

2.3 Multilayer CCR

The multilayer CCR is an extension of the CCR which integrates texture and colour into a single model [6]. The key point is to describe the colour content of an image through a suitable set of its most representative colours (*palette*), and then to split the image into a stack of binary layers, one for each colour of the palette. To this end, each pixel is assigned an index encoding the colour of the palette which is most perceptually similar to the pixel colour, and then it is set to one in the layer corresponding to this index, and to zero in the re-

maining layers. The overall feature vector for each pixel is formed by the codes of the corresponding binary patterns that occur in each layer.

There are two main approaches to generate the reduced colour palette. On the one hand, an image-independent palette can be generated by *colour space quantization*, which can be straightforwardly implemented by dividing the RGB colour cube into equally-sized parallelepipeds. This implies that the resulting palette is invariable, i.e., the same palette is used for all the images to be processed. This approach has been successfully applied to colour texture classification [6]. Colour space quantization can be generalized to multispectral imaging by partitioning the n -dimensional space into equal-sized buckets. On the other hand, an image-dependent palette can be generated through *colour clustering*. In doing so, the palettes corresponding to

different input images are different because they depend on the colour distribution of each image. We tested both approaches and found that colour clustering significantly outperforms uniform colour space quantization. Based on the results of this preliminary study we adopted the latter approach, using one of the most popular colour clustering implementations: the k -means algorithm. Once the colour palette is generated, the colour triplet –or n -tuple in case of multispectral imaging– of each pixel is replaced by the index of the colour in the palette that most closely resembles the original colour. This process is referred to as *colour indexing*. To that end, it is necessary to quantitatively define the perceptual “closeness” of a pair of colours. In this work we used the euclidean distance between the corresponding colour triplets (or n -tuples).

3 DESCRIPTION OF THE METHOD

The segmentation process is divided into two phases: training and testing. The first step of the training phase consists in generating a colour palette through either uniform colour space quantization or colour clustering, as described in Section 2.3. Henceforth the number of palette colours is referred to as N . We found that colour clustering outperforms uniform colour space quantization in roughly 20 percentage points of segmentation accuracy, and hence this was the approach we adopted. To generate the colour palette, the n -tuples of the original image were fed to the k -means clustering algorithm, where n denotes the number of bands of the image. Then, the 3×3 square neighbourhoods are transformed into circular neighbourhoods through bilinear interpolation (see Section 2.2), and subsequently, each pixel is assigned the index of the closest colour in the palette. It is useful to note that replacing the 3×3 window by a circular neighbourhood in a colour image involves n interpolations of the values of the neighbours that do not lie exactly on the original pixels positions, i.e. the bilinear interpolation has to be performed over each channel separately.

The next step consists in assigning a feature vector to each pixel. For this aim, the indexed circular patterns are split into N binary circular patterns, one binary pattern for each colour of the palette. A pixel that has been assigned the index i in the indexed pattern takes a value of 1 in the binary pattern corresponding to colour i , and 0 in the rest of the binary patterns. Each of the N circular binary patterns is assigned the code of the corresponding rotationally invariant patterns. The pixel is finally

assigned a feature vector which is made up of the codes of the corresponding elementary patterns. The overall procedure is schematically depicted in Figure 1.

Once the feature vectors of the pixels of the train images have been computed, the last step consists in choosing an appropriate classifier. It is well-known that the classifier performance is strongly dependent of the specific domain of the application. In view of the limited *a priori* knowledge we had, we considered that it would be worthy to try different classifiers in order to choose the best suited for our particular application. To accomplish this task we used the Waikato Environment for Knowledge Analysis (WEKA¹) workbench [29]. The error rates obtained in these trials were very similar, independently of the classification scheme. In view of this, we chose the RandomTree algorithm [29], due to its inherent ability to manage with the kind of features we propose in this paper and its reasonable computational complexity.

In the testing phase we have to compute rotation-invariant multilayer CCR features for each pixel of the image to be processed following the method just described, with the only difference that in this case we have to use the palette generated in the training phase. These features are then submitted to the RandomTree classifier which has been previously trained. The classifier returns a class label for each pixel of the test image. In order to make a realistic estimation of the generalization error, the image used for testing should be different from the image used for training.

Finally, to evaluate the accuracy of the method,

¹<http://www.cs.waikato.ac.nz/ml/weka/>

segmentation results are shown as indexed maps, where the pixel labels assigned by the classification algorithm are colour-coded for visualization purposes. Besides these maps, we computed sev-

eral figures of merit to quantitatively assess performance, namely success rate, precision and sensitivity, which will be described in Section 5.

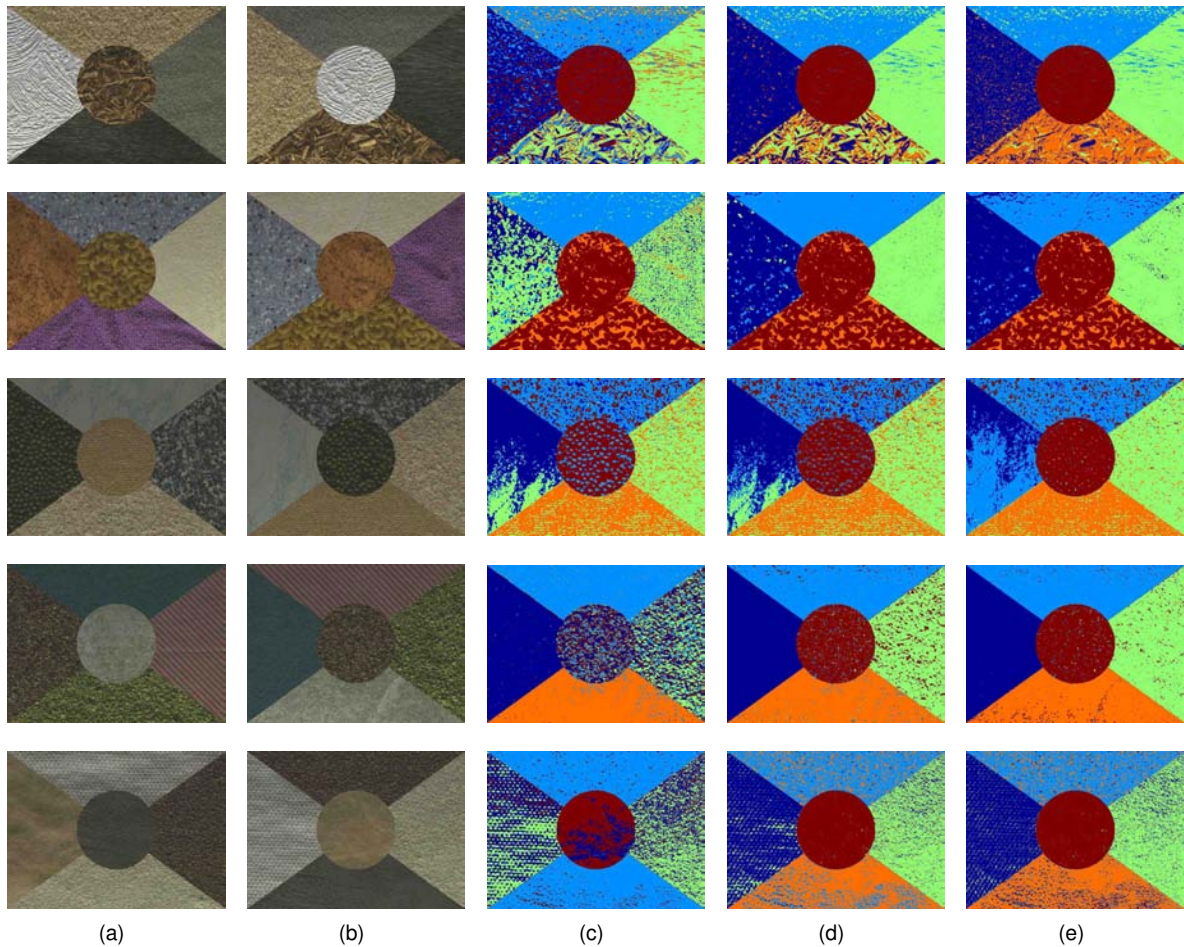


Figure 2: Synthetic mosaics of OuTex textures: (a) train images, and (b) test images, and segmentation results obtained using a palette of: (c) 5 colours, (d) 15 colours, and (e) 35 colours. Each row corresponds to a different mosaic.

4 BENCHMARK DATA

In order to assess the validity of the proposed method, we applied the rotation-invariant multilayer CCR model to the segmentation of two different types of images, which are briefly described in the following subsections.

4.1 Texture mosaics

The first group is composed of synthetic mosaics of texture images taken from the OuTex database [21]. OuTex images are commonly used by the computer vision community as an evaluation framework for texture analysis. We selected

a subset of 25 textures of the group *inca 100dpi* from the OuTex library. Five different mosaics of 746×538 pixels have been generated, each mosaic being formed by five different textures, as shown in Figure 2. It is important to note that the mosaics used for training contain the same textures than the mosaics used for testing, but as one can readily see from Figures 2(a) and 2(b), the patches of a given texture in the train mosaic and the test mosaic correspond to non overlapping samples of the original OuTex texture. The mosaics were created this way in order to keep the training and testing stages independent of each other, and hence, to

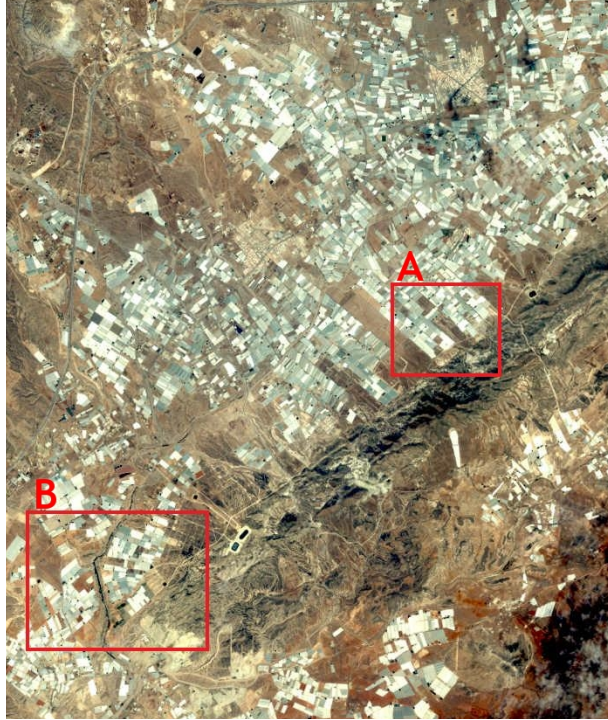


Figure 3: Study site areas from Ikonos-2

Table 1: Percentage of correctly classified pixels in OuTex mosaics. The mosaic number refers to the corresponding row in Figure 2

| Mosaic | Number of colours | | |
|--------|-------------------|-------|-------|
| | 5 | 15 | 35 |
| 1 | 70.58 | 83.73 | 89.90 |
| 2 | 62.94 | 80.82 | 80.16 |
| 3 | 74.40 | 75.64 | 77.64 |
| 4 | 75.23 | 93.84 | 96.92 |
| 5 | 53.74 | 84.38 | 85.20 |

avoid underestimation of the generalization error.

4.2 Satellite imagery

The mosaics described above are composites of textures imaged in a highly controlled laboratory environment. In real world applications, it is uncommon to achieve these ideal conditions. Therefore, in order to further validate the proposed approach, we used a second dataset formed by high resolution Ikonos-2 satellite imagery –R, G, B and NIR bands– of Campo de Níjar, in Almería province, south-eastern Spain (see Figure 3). Two non overlapping subimages of 498×465 pixels and 634×594 pixels have been cropped from the whole image, one for training and one for testing. These

subimages are shown in Figure 4(a). Our goal is to demonstrate the effectiveness of the rotation-invariant multilayer CCR features in the detection of areas covered by plastic greenhouses. Greenhouse agriculture located in the southeast of Spain concentrates the highest production of vegetables in the Iberian peninsula. The economic strength of this sector has caused a rapid and uncontrolled greenhouse surface expansion, and as a consequence, environmental threats have arisen [2]. A proper way to measure and control the covered surface and its evolution through time is being increasingly demanded by the government. The application of remote sensing and image processing techniques would be a helpful tool for the agricultural authorities to manage the greenhouse farming sector.

5 EXPERIMENTAL RESULTS AND DISCUSSION

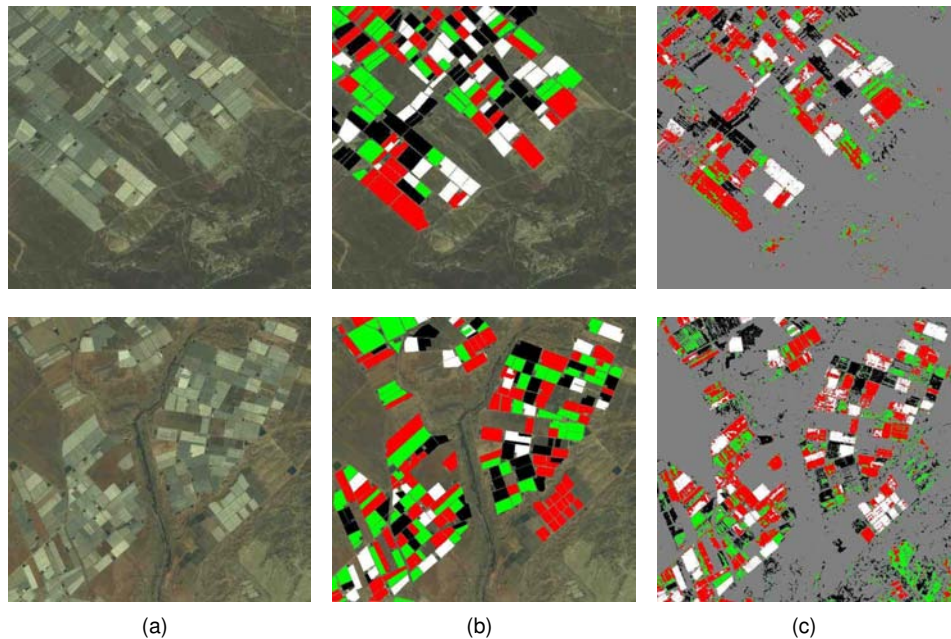


Figure 4: (a) Cropped subimages from Fig. 3, (b) manually delineated ground reference data, and (c) detected greenhouses. First row corresponds to region A, and second row corresponds to region B.

We performed a set of segmentation experiments using the rotation-invariant multilayer CCR over the two datasets described in the preceding section. For this purpose we implemented our own image processing algorithms in Matlab. We first studied the influence of colour quantization on the performance of the proposed approach. We found that segmentation accuracy is strongly affected by the number of colours that form the reduced colour palette. Figures 2(c) - 2(e) –corresponding to a palette of 5, 15 and 35 colours, respectively—clearly show that the greater the palette size, the higher the segmentation accuracy, as one could expect. However, it should be noted that in practice there is an upper limit for the number of colours, since computational overhead grows exponentially with the palette size. In addition to the visual assessment provided by Figure 2, we computed the percentage of correctly classified pixels as a figure of merit for the segmentation. Quantitative results obtained for OuTex mosaics are gathered in Table 1. From both this table and Figures 2(c) - 2(e) we can see that there is a great spread in performance: a success rate close to 100% can be achieved, but there are also cases in which considerable confusion between classes occurs. This fact is most evident in coarse textures and in mosaics that contain two or more patches with similar visual properties.

As we have previously said (Sect. 3), we tested different classification algorithms implemented in the WEKA suite in order to choose the most suitable classifier. From this trials we found that classification results were fairly independent of the algorithm

employed. Indeed, Table 3 makes it apparent that there are little variations in success rate from one algorithm to another. We chose the RandomTree algorithm [29] since this classifier performs well over our datasets and has a relatively moderate computational complexity.

The second part of the experimental activity focuses on the satellite imagery described in Section 4.2. Herein the objective is to discriminate the greenhouses from the rest of elements in the image, such as soil, roads, water pools, etc. From Figure 4(a) one can easily see that the visual appearance of the greenhouses may vary appreciably from one instance to another. Such differences should not be surprising, since the spectral signature of plastic strongly depends on factors like viewpoint, chemical composition and age [1]. Considering all the greenhouses as belonging to a unique class would lead to under-detection. Thus, we have grouped the greenhouses into four types from mere visual inspection. Figure 4(b) shows the manually defined ground reference data, and Figure 4(c) shows segmentation results. Careful observation of the lower rightmost corner of region A reveals the presence of abandoned greenhouses, which will likely introduce classification errors. Apart from the percentage of correctly classified pixels, we computed two additional figures of merit: sensitivity and precision. *Sensitivity* measures the proportion of correctly classified target pixels. *Precision* is the number of true positives divided by the total number of elements labeled as positives, so it can be regarded as a measure of exactitude [29]. The numerical results are gathered

Table 2: Numerical results (expressed in percentage) obtained for Ikonos-2 satellite imagery

| Test area | Success rate | Sensitivity | Precision |
|-----------|--------------|-------------|-----------|
| A | 86.68 | 65.71 | 84.06 |
| B | 82.38 | 81.01 | 69.53 |

Table 3: Pixel classification accuracies obtained with different classifiers over OuTex dataset with a palette of 15 colours obtained through k -means colour clustering.

| WEKA algorithm | Success rate (%) |
|------------------------|------------------|
| Bagging (J48) | 85.32 |
| BayesianNetwork | 83.33 |
| MultilayerPerceptron | 84.07 |
| NaiveBayes | 80.15 |
| RandomTree | 85.30 |
| RandomForest | 85.35 |
| Support Vector Machine | 80.51 |

in Table 2. It should be noted that in the calculation of these figures of merit only two classes are considered: ‘greenhouse’ and ‘background’, and therefore, all the pixels labeled as greenhouse – irrespective of the particular type of greenhouse – are merged into a single class.

In this experiment, the palette size was set to 15 since we found that this value is a good tradeoff between segmentation accuracy and computational burden. Although Ikonos-2 imagery consists of 4 bands (R, G, B and NIR), we only used the RGB bands and neglected the NIR band. This decision was based on the fact that including the infrared band produces only a slight improvement in segmentation accuracy, whereas provokes a significant raise of the computational overhead.

For comparison purposes, we tested our benchmark data with two different methods: Bayesian classifier and AdaBoost algorithm. In both cases each pixel is represented by either a RGB triplet for the OuTex dataset or a RGB+NIR quartet for the Ikonos-2 dataset. The *Bayesian classifier* is a classical, well-known classifier that assigns to each pixel the class with the maximum a posteriori probability [9]. Our implementation relies on the hypothesis that the probability density function of pixel intensities is a multivariate Gaussian distribution [11]. *Spatial AdaBoost* is a state-of-the-art

machine learning technique for contextual supervised image classification of land-cover categories of geostatistical data [18, 19]. The method classifies a pixel through a convex combination of a log posterior probability at the current pixel and averages of log posteriors in various neighbourhoods of the pixel. Weights for the log posteriors are tuned by minimizing the empirical risk based on the exponential loss function. In our implementation we used the inverse of the Mahalanobis distance as weak classifier. The results of these tests are shown in Figures 5(a) and 5(b), and Table 4.

The noisy aspect of Figure 4(c) indicates that most of the incorrectly classified pixels belong to small speckles or even are isolated pixels. This happens because the segmentation algorithm works on a per-pixel basis, i.e., each pixel is assigned a class label based exclusively on its feature vector. As described in Section 2.3, this feature vector only takes into account a 3×3 pixel neighbourhood, disregarding the spatial relationships with more distant pixels. One could reasonably expect that removing the small isolated clusters of wrongly classified pixels from the segmented image would increase accuracy. To this end we successfully implemented diverse morphology and smoothing filters, which gave rise to improved outcomes, as can be ascertained from Figure 5(c) and Table 4.

6 CONCLUSIONS

In this paper we presented the rotation-invariant multilayer CCR descriptor for colour texture. The validity of the proposed model has been demonstrated through image segmentation of mosaics of OuTex textures as well as greenhouse detection from high resolution Ikonos-2 satellite imagery. Experiments show that the proposed colour texture features have high discriminative power and yield

increased accuracy compared to other segmentation methods, such as the Bayesian classifier and Spatial AdaBoost. Furthermore, the proposed feature set is robust, since similar segmentation results are obtained by employing different classifiers. The obtained results suggest that the application of a post processing stage to remove noise may substantially improve classification accuracy.

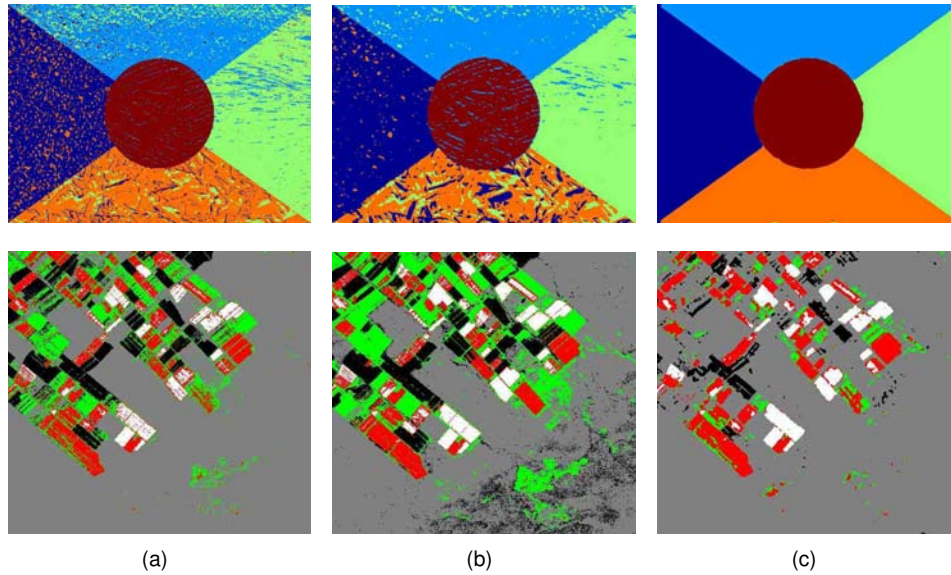


Figure 5: Segmentation results obtained using: (a) Bayesian classifier, (b) Spatial AdaBoost, and (c) rotation-invariant multilayer CCR, RandomTree classifier and median filtering. The test images corresponding to the first and second rows are Figure 2(b) (second row) and Figure 4(a), respectively.

Table 4: Percentage of correctly classified pixels for different segmentation methods

| Test image | Bayes | Spatial AdaBoost | Our approach | |
|-------------------------|-------|------------------|-------------------|----------------|
| | | | without filtering | with filtering |
| Figure 2(b) , first row | 85.52 | 89.73 | 89.90 | 99.79 |
| Figure 4(a) | 85.28 | 75.35 | 86.68 | 96.45 |

References

- [1] F. Agüera, M. A. Aguilar, and F. J. Aguilar. Detecting greenhouse changes from Quickbird imagery on the Mediterranean coast. *International Journal of Remote Sensing*, 27:4751–4767, 2006.
- [2] F. Agüera, F. J. Aguilar, and M. A. Aguilar. Using texture analysis to improve per-pixel classification of very high resolution images for mapping plastic greenhouses. *ISPRS Journal of Photogrammetry and Remote Sensing*, 63:635–646, 2008.
- [3] M. A. Akhloufi, W. B. Larbi, and X. Maldague. Framework for color-texture classification in machine vision inspection of industrial products. In *Proceedings of the IEEE International Conference on Systems, Man and Cybernetics, 2007. ISIC*, pages 1067–1071, Montreal, Canada, October 2007.
- [4] V. Arvis, C. Debain, M. Berducat, and A. Benassi. Generalization of the cooccurrence matrix for colour images: application to colour texture classification. *Image Analysis and Stereology*, 23(3):63–72, 2004.
- [5] F. Bianconi, A. Fernández, E. González, and F. Ribas. Texture classification through combination of sequential colour texture classifiers. In Luis Rueda, Domingo Mery, and Josef Kittler, editors, *Progress in Pattern Recognition, Image Analysis and Applications. Proceedings of the 12th Iberoamericann Congress on Pattern Recognition (CIARP 2007)*, volume 4756 of *Lecture Notes in Computer Science*, pages 231–240. Springer, 2008.
- [6] F. Bianconi, A. Fernández, E. González, D. Caride, and A. Calviño. Rotation-invariant colour texture classification through multilayer CCR. *Pattern Recognition Letters*, 30(8):765–773, 2009.
- [7] F. Bianconi, A. Fernández, E. González, and J. Armesto. Robust colour texture features based on ranklets and discrete Fourier transform. *Journal of Electronic Imaging*, 18:043012–1–8, 2009.
- [8] A. Drimborean and P. F. Whelan. Experiments in colour texture analysis. *Pattern Recognition Letters*, 22(10):1161–1167, 2001.

- [9] R. O. Duda, P. E. Hart, and D. G. Stork. *Pattern Classification*. Wiley-Interscience, 2001.
- [10] A. Fernández, O. Ghita, E. González, F. Bianconi, and P. F. Whelan. Evaluation of robustness against rotation of LBP, CCR and ILBP features in granite texture classification. *Machine Vision and Applications*, 2010. To appear.
- [11] R. C. González and R. E. Woods. *Digital Image Processing*. Pearson Prentice Hall, 2008.
- [12] R. M. Haralick. Statistical and structural approaches to texture. *Proceedings of the IEEE*, 67(5):786–804, 1979.
- [13] D. Iakovidis, D. Maroulis, and S. Karkanis. A comparative study of color-texture image features. In *Proceedings of the 12th International Workshop on Systems, Signal and Image Processing (IWS-SIP 2005)*, pages 205–209, Chalkida, Greece, September 2005.
- [14] A. Khotanzad and J. Bennett. A classification methodology for color textures using multispectral random field mathematical models. *Mathematical and Computational Applications*, 11:111–120, 2006.
- [15] E. V. Kurmyshev and M. Cervantes. A quasi-statistical approach to digital binary image representation. *Revista Mexicana de Física*, 42(1):104–116, 1996.
- [16] T. Mäenpää and M. Pietikäinen. Classification with color and texture: jointly or separately? *Pattern Recognition*, 37(8), 2004.
- [17] M. Mirmehdi and M. Petrou. Segmentation of color textures. *IEEE Transactions on Pattern Analysis and Machine Intelligence*, 22(2):142–159, 2000.
- [18] R. Nishii and S. Eguchi. Robust supervised image classifiers by spatial AdaBoost based on robust loss functions. In *Image and Signal Processing for Remote Sensing XI*, volume 5982 of *Proceedings of SPIE*, page 59820D, October 2005.
- [19] R. Nishii and S. Eguchi. Supervised image classification by contextual AdaBoost based on posteriors in neighborhoods. *IEEE Transactions on Geoscience and Remote Sensing*, 43(11):2547–2554, 2005.
- [20] T. Ojala, M. Pietikäinen, and T. Mäenpää. Multiresolution gray-scale and rotation invariant texture classification with local binary patterns. *IEEE Transactions on Pattern Analysis and Machine Intelligence*, 24(7):971–987, 2002.
- [21] T. Ojala, M. Pietikäinen, T. Mäenpää, J. Viertola, J. Kyllönen, and S. Huovinen. Outex - new framework for empirical evaluation of texture analysis algorithms. In *Proceedings of the 16th International Conference on Pattern Recognition (ICPR'02)*, volume 1, pages 701–706, Quebec, Canada, 2002. IEEE Computer Society.
- [22] C. Palm. Color texture classification by integrative co-occurrence matrices. *Pattern Recognition*, 37(5):965–976, 2004.
- [23] T. Randen and J. H. Husøy. Filtering for texture classification: A comparative study. *IEEE Transactions on Pattern Analysis and Machine Intelligence*, 21(4):291–310, 1999.
- [24] R. E. Sánchez-Yáñez, E. V. Kurmyshev, and F. J. Cuevas. A framework for texture classification using the coordinated clusters representation. *Pattern Recognition Letters*, 24(1-3):21–31, 2003.
- [25] R. E. Sánchez-Yáñez, E. V. Kurmyshev, and A. Fernández. One-class texture classifier in the CCR feature space. *Pattern Recognition Letters*, 24(9-10):1503–1511, 2003.
- [26] K. Y. Song, J. Kittler, and M. Petrou. Defect detection in random colour texture. *Image Vision and Computing*, 14(9):667–683, 1996.
- [27] T. S. C. Tan and J. Kittler. Colour texture analysis using colour histogram. *IEE Proceedings - Vision, Image and Signal Processing*, 141(6):403–412, December 1994.
- [28] M. Tuceryan and A. K. Jain. Texture analysis. In C. H. Chen, L. F. Pau, and P. S. P. Wang, editors, *Handbook of Pattern Recognition and Computer Vision (2nd Edition)*, pages 207–248. World Scientific Publishing, 1998.

- [29] I. H. Witten and E. Frank. *Data Mining: Practical Machine Learning Tools and Techniques*. Morgan Kaufmann Series in Data Management Systems. Morgan Kaufmann, second edition, 2005.
- [30] G. van de Wouwer, P. Scheunders, S. Livens, and D. van Dyck. Wavelet correlation signatures for color texture characterization. *Pattern Recognition*, 32(3):443–451, 1999.
- [31] X. Xie and M. Mirmehdi. A galaxy of texture features. In M. Mirmehdi, X. Xie, and J. Suri, editors, *Handbook of texture analysis*, pages 375–406. Imperial College Press, 2008.